A Magnetic Bio-Inspired Soft Carrier as a Temperature-Controlled Gastrointestinal Drug Delivery System

Christoff M. Heunis,* Zhuoyue Wang, Gerko de Vente, Sarthak Misra, and Venkatasubramanian Kalpathy Venkiteswaran

Currently, gastrointestinal bleeding in the colon wall and the small bowel is diagnosed and treated with endoscopes. However, the locations of this condition are often problematic to treat using traditional flexible and tethered tools. New studies commonly consider untethered devices for solving this problem. However, there still exists a gap in the extant literature, and more research is needed to diagnose and deliver drugs in the lower gastrointestinal tract using soft robotic carriers. This paper discusses the development of an untethered, magnetically-responsive bio-inspired soft carrier. A molding process is utilized to produce prototypes from Diisopropylidene-1,6-diphenyl-1,6-hexanediol-based Polymer with Ethylene Glycol Dimethacrylate (DiAPLEX) MP-3510 - a shape memory polymer with a low transition temperature to enable the fabrication of these carriers. The soft carrier design is validated through simulation results of deformation caused by magnetic elements embedded in the carrier in response to an external field. The thermal responsiveness of the fabricated prototype carriers is assessed ex vivo and in a phantom. The results indicate a feasible design capable of administering drugs to a target inside a phantom of a large intestine. The soft carrier introduces a method for the controlled release of drugs by utilizing the rubbery modulus of the polymer and increasing the recovery force through magnetic actuation.

C. M. Heunis, G. de Vente, S. Misra, V. K. Venkiteswaran
Surgical Robotics Laboratory
Department of Biomechanical Engineering
University of Twente
Enschede 7500 AE, The Netherlands
E-mail: c.m.heunis@utwente.nl
Z. Wang, S. Misra
Department of Biomedical Engineering
University of Groningen and University Medical Centre Groningen
Groningen 9713 GZ, The Netherlands

The ORCID identification number(s) for the author(s) of this article can be found under https://doi.org/10.1002/mabi.202200559

1. Introduction

Acute gastrointestinal (GI) bleeding is a potentially life-threatening abdominal emergency that remains a common cause of hospitalization. Multiple lesions can occur virtually anywhere in the gastrointestinal tract. In the lower GI tract (particularly in the transverse colon), hemorrhages often require surgery, with as many as a million hospitalizations annually worldwide and a mortality rate of up to 10%.[1] The evaluation of acute lower GI bleeding in patients involves a diagnostic study, followed by the treatment of the site of bleeding utilizing a flexible sigmoidoscopy. The most common treatment for bleeding is initiated by the intravenous delivery of proton pump inhibitors—aimed at the prolonged reduction of stomach acid production.[2] This lengthy process is then followed by the guidance of an endoscope to the bleeding site for further diagnosis and treatment.[3] Even though tethered endoscopic techniques have improved the management of GI bleeding and have been considered the norm,[4] such procedures are still accompanied by inherent risks, such as re-bleeding, discomfort to the patient, and perforation of the abdominal wall.[5,6] An additional medical drawback is that some regions of the GI tract, such as the small bowel, remain unreachable. Specifically, for the administration of drugs that exhibit a burst release (a high initial concentration and low adequate time), this inaccessibility results in the unwanted distribution of the drugs to healthy tissues.

A promising approach to solve these challenges is to concentrate on the potential of untethered devices, since they require no flexible tubes to be actuated. Extensive efforts have focused on developing such devices to treat GI bleeding.[7] For instance, systems inspired by creatures in nature have attracted the attention of researchers owing to their effective locomotion mode and high environment adaptability during motion. Examples include snail-like soft robots,[8] sipunculid worms,[9] and inchworms.[10,11] Researchers have mimicked such creatures primarily by designing self-folding robots with a soft and deformable nature that demonstrate high adaptivity to confined spaces within the body.[12–14] Moreover, such devices can be

ingested orally or easily inserted into body orifices owing to their size and soft structures.

In the last decade, untethered thermo-magnetic responsive systems have been developed owing to the research of responsive materials such as poly(N-isopropyl acrylamide) hydrogels[15] and shape memory polymers (SMPs).[16,17] These polymers are lightweight and have high strain and shape recovery abilities. Regarding their utilization *in vivo*, the inherent flexibility and adaptability of SMPs are beneficial, considering that the anatomical environment constantly experiences external physiological disturbances. These abilities make them popular for interdisciplinary research—primarily to diagnose and treat diseases. SMPs are characterized by their ability to undergo controllable and reversible physical or chemical change under exposure to external stimuli, such as chemicals, light, and magnetic fields.[18] This ability allows for tuning their physical and chemical polymeric properties, including their elasticity, polarity, and strength.[19]

Thermal triggering under biologically relevant conditions has been increasingly investigated as a remote triggering mechanism for shape change. For example, Leong *et al.* showed that deformable devices could be actuated even while spatially separated.[20] They demonstrated diverse functions, such as picking up objects *in vivo* and removing cells from tissue during *in vitro* biopsies. Liechty *et al.* proposed drug delivery SMPs able to transform when exposed to solvents.[21] They showed that the polymer would dissolve in a thermally-suitable aqueous environment. In turn, this functionality can be used to trigger drug administration.

Even though current shape-memory devices provide a seamless way of generating shape change, their efficacy relies highly on the environment in which they are designed to function. GI bleeding occurs in a challenging, deep-seated anatomical environment. Therefore, drug administration should be controlled on-site and inhibit the excessive spreading of the drug to surrounding tissues. Furthermore, most thermally-responsive polymers cannot undergo a shape transformation beyond their permanent states in the body without the assistance of an external active heating element. Since such temperatures will damage the inner lining of the intestinal wall, their utilization is purely experimental. It limits their working environments and function within the GI tract. To bypass this need, magnetic triggering can be considered a suitable complementary stimulus.

Numerous *in vivo* investigations have been conducted to evaluate the clinical feasibility of magnetic biomedical robotic devices for various applications such as biopsies, pick and place, and drug delivery.[22,23] These devices can be used to retrieve tissue samples from within the body for pathological examination, such as metallic microgrippers[24] or micro-drillers.[25] Additionally, these devices can deliver drugs or other therapeutic agents to a targeted site within the body, including bacterium[26] and microswimmers.[27] However, a significant challenge associated with these devices is the low stiffness of their gripping components, which can negatively impact their performance. Effective drug delivery requires a secure holding mechanism to ensure the safe transport and targeted delivery of therapeutic agents. For instance, the hinges of the magnetic theragrippers presented by Liu *et al.* in an *ex vivo* pick and place study were reported to be fragile, resulting in grippers with limited capacity to secure drug particles and an increased likelihood of particle loss.[28] Breger

et al. improved on this approach by developing origami-inspired, and stimuli-responsive structures capable of bi-directional folding based on temperature and magnetics.[29] On-site origami sheet self-folding magnetic devices were introduced by Miyashita *et al.*,[30] who demonstrated their ability to walk, swim, and move objects. Ahmed *et al.* discuss a range of applications for such devices, including tissue scaffolds, drug delivery, and implants.[31] Taking inspiration from crawlers, Lu et al. developed a flexible, untethered soft millirobot with obstacle-crossing abilities.[32] Ze *et al.* improved on this concept by creating a magnetically actuated origami crawler that stores and releases drugs while navigating severely confined spaces.[33] This crawler could overcome obstacles caused by contact between tissues and organs that can hinder its motion and function. However, these crawlers only consisted of a single material containing a simple geometry and magnetization profile. This limits their functionality as biomedical devices intended for multiple uses. Zhang *et al.* aimed to mitigate this by investigating arbitrary multi-material compositions of soft carriers.[34] They were able to demonstrate peristaltic motions, transportation, and delivery. Nonetheless, retrieval of the carrier was still lacking in their experimental stages of development. Wang *et al.* proposed fabricating such carriers with dissolvable and biocompatible segments.[35] This allows the carrier to pass through the GI tract of the patient without additional risks of bleeding.

Star-shaped devices have been proposed as a solution to address the challenge of low stiffness in gripping components of biomedical magnetic robotic devices. These devices feature multiple arms or arm-like structures that can securely hold drug particles and minimize the risk of particle loss. The star-shaped design offers a larger surface area for drug containment, enabling the simultaneous delivery of multiple agents to a single target site, as reported by Ongaro *et al.*[36] Recently, Dunn *et al.* demonstrated the use of star-shaped grippers made of SMP and metal bilayer, which self-activate in response to elevated temperatures and can be directed using magnetic forces for tissue biopsy and retrieval.[37] However, further improvement is required regarding the guidance of the grippers and a consistent retrieval method after completing their task.

In this study, we propose a magnetically-aided shape transformation approach that leverages the benefits of soft SMPs, bio-inspired design, and magnetic actuation to create a new class of soft carriers. Drawing inspiration from the behaviors of Sugar starfish (*Asterias rubens*), this paper presents a magnetically-actuated GI drug delivery soft carrier. The carrier is designed to mimic the dual-shape states of a starfish, as illustrated in **Figure 1**a. The SMP-based soft carrier only responds to body temperature during shape transformation, in contrast to transition temperatures higher than 40°C, requiring no active heating element. This makes it a safer solution than current SMP soft robots while enabling its remote actuation, drug transport, and administration.

The reason for choosing the starfish-shaped configuration is three-fold: 1) it enables the grasping and release of a drug, 2) it allows for shape transformation and adaptation, and 3) the surface-to-volume ratio of the carrier can be drastically changed to allow for insertion via natural orifices. This miniaturized bio-inspired device should be able to approach a target site, demonstrate a one-way shape transformation in a complementary fashion, and
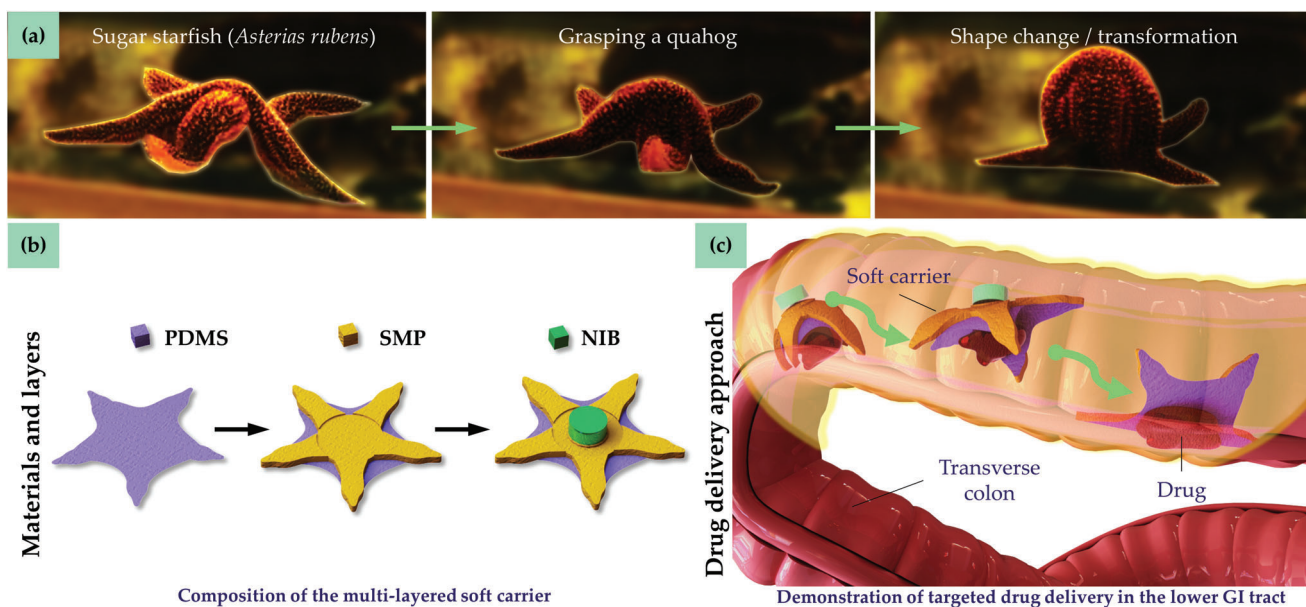
**ADVANCED
SCIENCE NEWS**

www.advancedsciencenews.com

**[M]acro-
molecular
Bioscience**

www.mbs-journal.de

Figure 1. This study utilizes a temperature-sensitive mechanism to design a magnetic bio-inspired soft carrier. a) This carrier draws inspiration from the body of a sugar starfish (*Asterias rubens*) during hunting. It consists of a central disc and multiple radiating arms capable of pulling the starfish around an object (e.g., a quahog). b) The device consists of a multi-layered structure - each layer constituting a different purpose. First, a polydimethylsiloxane (PDMS) membrane confines the drug at the target site. Next, a one-step dual-shape memory polymer (SMPs) is utilized for thermally-induced shape transformation. Finally, a nickel-plated neodymium (NIB) disc magnet is secured in the center of the SMP body to allow for transformation beyond the permanent SMP shape and magnetic guidance to the target site. c) Such a temperature-controlled gastrointestinal drug delivery system can change shape at the target site, allowing for the controlled release of temperature-sensitive drugs.

release a drug at the site. It should maneuver through a small orifice akin to the tiny organs or vessels and be wirelessly controlled from outside the body. This device targets high-risk, challenging interventions at remote sites deep inside the human body that cannot be tackled using minimally invasive surgical techniques. In the experiments presented herein, the feasibility of body heat as the primary external trigger mechanism for shape change and drug dissolution is assessed. Our primary goal is to report efforts to enhance the rubbery modulus and increase the recovery force by incorporating magnetic elements. The clinical feasibility of the mechanisms for application within the GI tract is estimated in terms of restrictions in size and functionality using mathematical and computer-aided modeling. Secondary to this goal, we demonstrate the feasibility of imaging this soft carrier using computed tomography angiography (CTA) and a traditional gastroscope.

2. Results and Discussion

We simulate, design, and assemble a soft multilayer carrier (Figure 1b) capable of targeted drug delivery within a realistic environment. It is made of a polydimethylsiloxane (PDMS) membrane, a layer of shape memory polymer (SMP), and a nickel-plated neodymium (NIB) disc magnet. The carrier is inserted into a clinically-relevant phantom resembling the GI tract at body temperature (Figure 1c). External fields produced by a permanent magnet influence the guidance and positioning of the carrier and, in addition, enable its subsequent deformation at the target. A gelatin-based biodegradable drug is delivered at a target location. A robust and timely shape recovery performance is achieved, followed by a different shape transformation phase in-

duced by the magnetic field (**Figure 2**a). According to [38], SMPs require at least three key factors to obtain a good shape memory effect: 1) Stimuli-responsive domains, 2) Sufficient elasticity, 3) A customized programming process. We propose a complementary addition—4) A suitable switching segment (Figure 2b). Such a segment allows for localized folding, concentrating shape change along creases that can be controlled. Our framework and modeling approach allows us to predict the shape fixity (Figure 2c) and drug release rates to ensure a controlled and on-site administration.

2.1. Device Concept and Modelling

As illustrated in **Figure 3**a, a 3D model is used for demonstrating the pseudoelasticity of the soft carrier situated within an air domain. In addition to the disc magnet on the soft carrier, a larger external magnet is included in the simulation. Both the magnet domains are modeled using separate built-in nodes and choosing their B–H curves as the constitutive relation. The magnetic interaction between the external and internal permanent magnets is then analyzed to initiate the magnetic shape morphing process (Figure 3b).

Magnetic interaction occurs between a (ferro)-magnetic dipole ($\boldsymbol{\mu} \in \mathbb{R}^3$) and the external field ($\mathbf{B}(\mathbf{p}) \in \mathbb{R}^3$) at a point ($\mathbf{p} \in \mathbb{R}^3$) in space.[39] In the presence of a permanent magnetic field, this dipole experiences a wrench ($\mathbf{W}_\mu \in \mathbb{R}^6$) comprising of force ($\mathbf{F}_\mu \in \mathbb{R}^3$) and torque ($\mathbf{T}_\mu \in \mathbb{R}^3$) components:

$$\mathbf{W}_\mu = \begin{bmatrix} \mathbf{F}_\mu \\ \mathbf{T}_\mu \end{bmatrix} = \begin{bmatrix} \nabla(\boldsymbol{\mu}^T \mathbf{B}(\mathbf{p})) \\ \boldsymbol{\mu} \times \mathbf{B}(\mathbf{p}) \end{bmatrix}. \tag{1}$$

**ADVANCED
SCIENCE NEWS**

www.advancedsciencenews.com
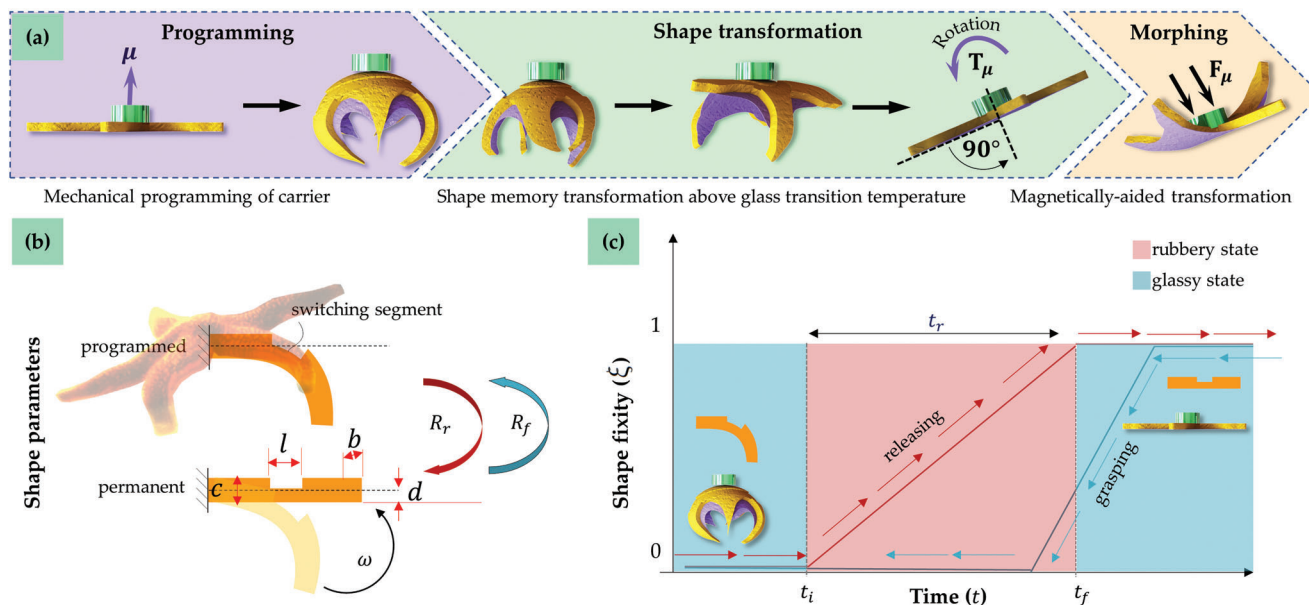
acro-
olecular
Bioscience

www.mbs-journal.de

Figure 2. We demonstrate complementary external trigger mechanisms (thermal and magnetic) for inducing shape transformation of our bio-inspired soft carrier. a) The carrier is fabricated in its initial (permanent) shape. Under mechanical loading, the carrier shape is programmed by submerging the permanent shape in water above its glass transition temperature (T_g). Below T_g, the material stays in its programmed state even after the load is removed, and residual deformation remains. The permanent shape is then retrieved by heating the material above T_g, followed by shape change through magnetic actuation. Furthermore, the dipole direction (μ) of the permanent magnet fixed to the body is perpendicular to the body surface. This allows for the maximum pressure on the carrier from an external magnet by a magnetic force (F_μ), and aligns the carrier due to an external magnetic torque (T_μ). b) The shape change of the carrier is based on transformations between its programmed and permanent shape phases. The design objective is to determine the shape recovery parameters (angular recovery rate (ω) corresponding to shape recovery rate (R_r) and shape fixity rate (R_f) for different beam widths (b), thicknesses (c), depth (d), and length (l). c) The phase transformation is described by the shape volume fraction variable (ξ). Blue arrows indicate the grasping transformation direction. When the material is programmed, the switching segment allows for localized transformation, inducing a bending moment of the entire arm. Red arrows indicate the transformation from an enclosed (programmed) shape to an open (permanent) shape. The soft carrier will be in its rubbery state starting at timestamp (t_i until t_f).
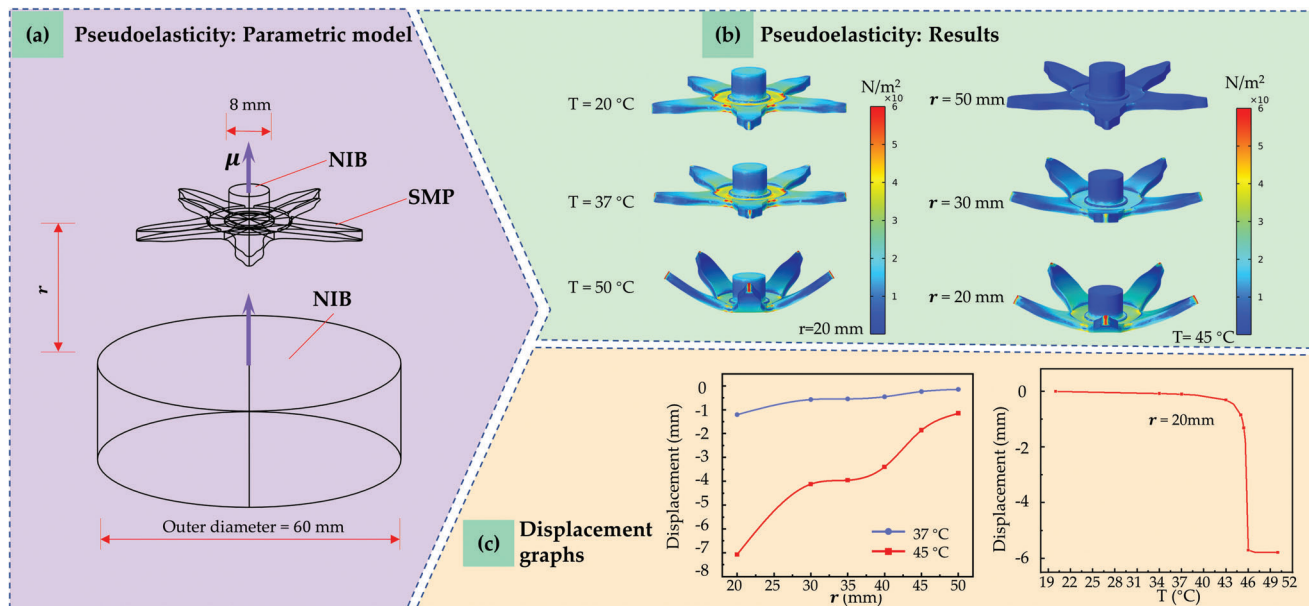

Figure 3. Simulations of deformation of the soft carrier in the presence of external magnetic fields and at different temperatures. a) Schematic diagram of the soft multilayer carrier and an external magnet. b) The simulation of the soft carrier mapping stress and deformations under two conditions: increasing the temperature (T) from 20 °C to 50 °C, and increasing the distance (r) between the magnets from 20 to 50 mm. c) Graphs showing displacement of the soft carrier under both conditions.

2200559 (4 of 9)

**ADVANCED
SCIENCE NEWS**

www.advancedsciencenews.com

**[M]acro-
molecular**
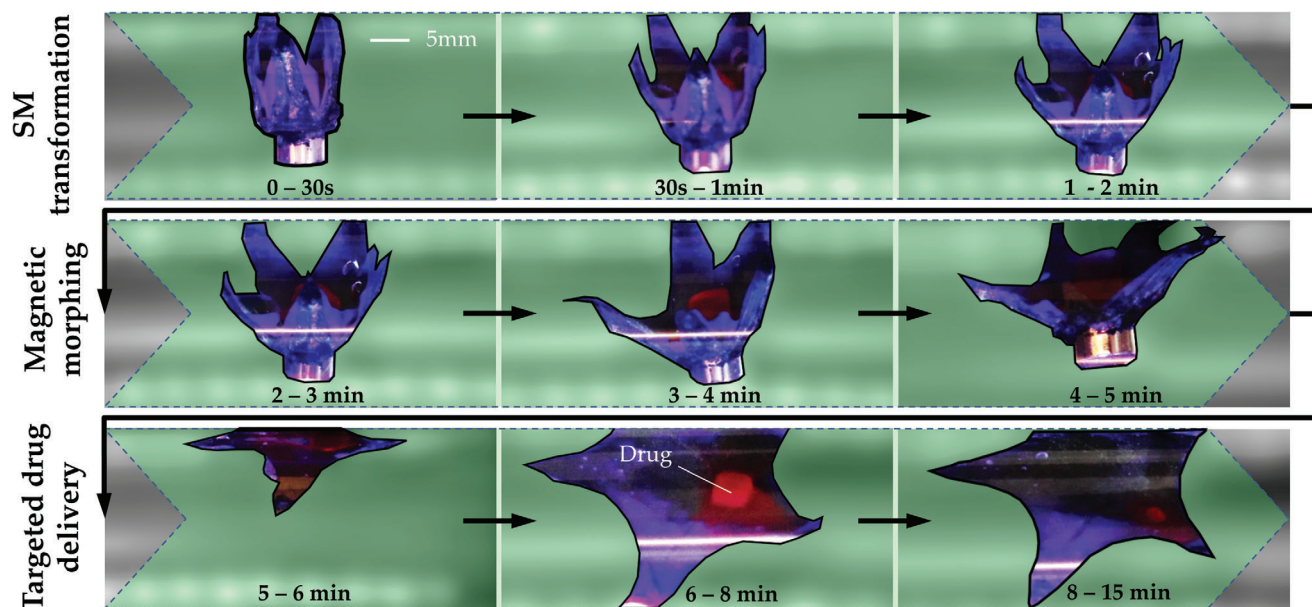Bioscience
www.mbs-journal.de

Figure 4. The experimental results. During the benchtop experiment, the carrier is moved wirelessly using an external permanent magnet to a target along a tube of 30 cm in length. Three phases are demonstrated during the experiment - shape memory (SM) transformation, magnetic morphing, and targeted drug delivery.

Coupled with the SMP, the soft carrier exhibits a strong response to changing temperature. When the distance between magnets (d) increases at set temperatures (37 °C and 45 °C), the carrier shows a non-linear change in deformation based on the constitutive model. Meanwhile, the carrier will deform dramatically when the temperature is above T_g (Figure 3c). It is noticeable that the carrier structure becomes signficantly softer and converges to the closed state as the temperature increases beyond T_g.

2.2. Material Composition

Therapeutic soft robotics design requirements are set up based on criteria from [40] so that the carrier can be inserted into a natural body orifice. A series of steps are taken to develop the soft carrier (Figure 1b). Our choice of a two-part potting compound, Diisopropylidene-1,6-diphenyl-1,6-hexanediol-based Polymer with Ethylene Glycol Dimethacrylate (DiaPLEX) MP3510 (SMP Technologies Inc., Shibuya City, Japan), for fabricating the polymer sheet is suitable for demonstrating a clinically-relevant SMP reacting to body temperature. The composite polydimethylsiloxane (PDMS) membrane served to enable controlled drug release and compression of the drug against the target site. This compression was achieved by means of an external magnet.

The use of soft materials has the advantage of reducing the forces applied to the colonic wall and consequently diminishing pain and discomfort to the patient during the procedure. Because of the low mechanical stiffness, a soft carrier can perform dexterous movements and follows the 3D-shaped contours of the colonic lumen, as illustrated by **Figure 4**.

2.3. Biodegradable Drug

The soft carrier is designed to transport a simulated drug consisting of a biodegradable gelatinous mixture. The bowel transit time is a factor that influences the chosen recovery rate of the polymer beam and the drug dissolution duration. The transit-time is patient-specific and can be estimated based on the patient's age, gender, body-mass index, and the anatomic measurements of the stomach and lower-GI tract.[41] This transit time limits the carrier's sustained and controllable release of drugs. Furthermore, the gastric cavity lends itself well for the prolonged residence of the carrier in case of oral ingestion.

The carrier was capable of achieving the desired outcome within the gastrointestinal tract of the benchtop phantom. The biodegradable drug cube dissolved fully after ~15 min, providing the operator time to actuate the soft carrier toward a target site. Furthermore, the composition and ratio of the drug mixture allow for the controlled release. Changing the ratio of the mixture changes the dissolvability as well as the mechanical properties of the drug. By adding glycerol, the cross-linking property of gelatin is diminished, which increases the solubility of the mixture. Based on this, we conducted a preliminary experiment. In this experiment, the dissolvability of the drug at body temperature is tested to control the dissolution time with the objective that the drug is released after the SMP has deformed.

2.4. Stimuli-Responsive Domains

Thermo-responsive SMPs possess shape morphing properties due to functional groups in their molecular structure. The functional groups or stimuli-responsive domains act as switches

2200559 (5 of 9)

**ADVANCED
SCIENCE NEWS**

www.advancedsciencenews.com

Macromolecular
Bioscience

www.mbs-journal.de

triggered when exposed to specific temperatures. In our case, a polymeric drug delivery system is designed to elicit spatiotemporal drug release capabilities. The glass transition temperature of the material enables the transition between the hard glassy state and the flexible rubbery state of the polymer. We define the temporary programmed, and permanent state in terms of the dual-shape memory cycle of the polymer.[42] The cyclic behavior of the polymer is illustrated in Figure 2c. The transition temperature (T_g) enables the transition between the hard glassy state and the flexible rubbery state of the polymer.

Ideally, SMPs designed for biomedical applications should have a sharp transition from glassy to rubbery state around a body temperature of 37 °C. The transition temperature of commercially-available materials for shape transformation extends over a large interval above far beyond this requirement, and the precise tuning of the transition temperature remains challenging.[43] The chosen material (DiaPLEX MP3510) has a transition temperature of 35 °C, making it suitable for use inside the human body.

2.5. Clinical Application

Since we propose the use of an untethered soft carrier in the colon, a suitable imaging modality must substitute an endoscopic camera to enable the clinical usage of the device. Therefore, two imaging modalities are used to demonstrate its geometry with relation to the life-size GI phantom. Using a video gastroscope, the carrier was clearly visible within the transverse colon phantom. The computed tomography angiography (CTA) scan showed no artefacts. This implies that the diagnosis and treatment can both be done using the same imaging modality.

Several magnetic manipulation-based clinical systems have demonstrated improved accuracy and control, making it a promising approach for *in vivo* applications. Swain *et al.* conducted the first human trial of wireless capsule endoscopy using a handheld magnet.[44] The magnetic forces can be brought in close proximity to the patient's abdomen. Keller *et al.* demonstrated a colon capsule embedded with a magnetic disc and a handheld magnet to control the capsule's movements.[45] Commercial systems include the handheld MiroCam-Navi (Intromedic Ltd., Seoul, Korea), MCE (Olympus Corp. and Siemens Healthcare), NaviCam (AnX Robotica, Wuhan, China), and the standing-type magnetic capsule endoscopy (JIFU Medical Technologies, Shenzen, China).[46] These systems provide comprehensive digestive tract navigation, and a non-invasive alternative to traditional endoscopic procedures, similar to the handheld magnetic actuation device demonstrated in this study. Magnetic resonance imaging (MRI) has also been proposed to guide and control magnetic manipulation devices.[47] MRI provides real-time visualization of the device and its location within the patient's body, allowing for precise manipulation and control through clinical instrumentation. However, it is important to note that the direction of magnetic fields within MRI scanners may limit actuation throughout the entire digestive tract. In particular, the homogeneous magnetic fields within the MR bore result in zero field gradients, as expressed in Equation 1. Consequently, the magnetic force ($\mathbf{F}_\mu$) is zero, making MRI unsuitable for our actuation strategy.

2.6. Shape Transformation

The untethered nature of a millimetre-scale robot restricts the level of control over its position and pose. The permanent magnet fitted in the center of the carrier allows operators to achieve control by using an external magnetic field as explained in (1). During our phantom experiments, we exploit $\mathbf{T}_\mu$ in order to align the dipole direction of the permanent magnet on the carrier with that of the external magnet (Figure 4). The magnetic force then allows us to increase the pressure of the carrier magnet against the SMP layer, which in turn compresses the drug against the intestinal wall.

The ability to transform its shape gives the presented device multi-functional capabilities. This approach can potentially transform interventional procedures and provide personalized and targeted minimally invasive solutions for challenging therapeutic applications. Other studies investigated the use of embedding such devices with electronics. Boyvat *et al.* demonstrated a battery-free wireless folding method for dynamic multi-joint structures, achieving addressable folding motions.[48] Faber *et al.* expanded on this approach by integrating synthetic elements inspired by biological wings.[49] This allowed the fabrication of '4D-printed' objects with programmable bio-inspired morphing functionalities.

By our estimates, body-sensitive trigger mechanisms increase design complexity of magnetic bio-inspired SMPs. Drug delivery applications primarily focus on controlled drug release enabling targeted drug delivery and minimizing large fluctuations in systemic drug concentrations. Controlled drug release from SMPs depends on the surface-to-volume ratio of the polymer. Consequently, the surface-to-volume ratio can be controlled by its shape morphing properties. The shape transformation ability of the carrier creates the opportunity to load the SMP-based system with drugs and fix them in a compact structure, making digestion or insertion through small orifices possible. Notwithstanding, challenges in fabricating devices with desirable dimensions and compliance remain crucial in follow-up studies. Further studies and experiments are needed to establish a clear relationship between polymer thickness and shape recovery prediction.

3. Conclusion

This study proposes a soft carrier that has the potential to enter the body through an orifice, reliably move to a remote site within the body while transporting and administering necessary drugs, and be subsequently retrieved. We envision this carrier to potentially have no adverse effects on the patient upon extraction, however, its risks will be assessed in a follow-up study. We investigate a unique approach to magnetically morph SMP structures using external forces to facilitate shape change. We identified and demonstrated several advantages of utilizing magnetic bio-inspired soft robots (carriers) as temperature-controlled gastrointestinal drug delivery systems. First, the carrier can be considered a disposable device. It has been designed according to the clinical practice guidelines for the FDA-allowed size, shape, and weight of commercial digestible devices. The device itself can be ingested orally or administered anally. This requires no surgical incisions, which has the potential to provide an improved

**ADVANCED
SCIENCE NEWS**

www.advancedsciencenews.com

[M]acro-olecular

Bioscience

www.mbs-journal.de

cosmetic outcome to the patient when compared to general surgical techniques.

According to the ISO 13485 standard for medical devices, factors like cleaning, disinfection, and maintenance, are not applicable for single-use disposable devices.[50] This will drastically reduce the health care costs compared to the traditional optical colonoscopy. It is important to conduct biocompatibility tests to confirm their safety for specific applications. PDMS is commonly used in medical devices and is generally considered safe for use in contact with the human body.[51] However, it is not intended for direct ingestion without an appropriate biocompatible coating, such as Polyethylene, as discussed by Li *et al.*[52] Furthermore, a biocompatible magnetic material such as iron oxide could be used for the magnetic component to reduce the risk of toxicity.[53] Alternatively, the surface of the magnet can be modified by applying a hydrogel coating that can reduce adhesion to the GI tract and minimize irritation. The soft robot should be able to overcome various challenges related to gastric residence time, various pH values, protective mucus layers, and differing diameters. Flexible or biodegradable materials are recommended for the SMP layer to prevent retention and the resulting clinical obstructive symptoms. Poly-vinyl alcohol (PVA) and Poly-lactic acid (PLA) are non-toxic and biologically degradable polymers. Although they have transition temperatures above 60 °C, they can be used as effective thermo- and water-responsive devices. Combining these materials with active, external heating elements should be considered. Finally, our chosen technique for fabricating the SMP lacks the accuracy for intricate designs. As an alternative to potting, additive manufacturing methods would enable more diverse shapes to be created and reduce lead time.

4. Experimental Section

Fabrication of the Soft Carrier: A series of steps were taken to develop the concept carrier (Figure 1). The two-part DiAPLEX MP3510 potting compound was used to fabricate a sheet of polymer representing the carrier's body. First, a silicone sheet bracket (80×80 mm) was made from Poly(methyl methacrylate) (PMMA) to aid the active disassembly of the polymer. Next, the DiaPLEX compounds were mixed within a single stage vacuum pump (Model VE-115, Vevor, Canada) to initiate the potting process within the bracket, resulting in a thin, 2 mm thick sheet of SMP. This thickness was chosen based on pre-experimental tests on polymer beams with varying thickness ($c = 1–4$ mm), each with a different depth ($d = 0.2c$, $0.3c$, and $0.5c$) as shown in Figure 2b. The recovery duration was measured for 12 different samples.

To guarantee dependable assessments of shape fixity versus recovery duration, each of the 12 samples underwent three measurements. The acquired data from the three measurements for each sample are analyzed to determine the mean and standard deviation of the shape fixity versus recovery duration. This repetition of measurements allowed to evaluate the repeatability and variability of the results. The results show that the $c = 2$ mm thickness among the samples exhibits the lowest error with standard deviations of 0.45, 0.65, and 0.20 mm s^{-1} for each respective depth. Corresponding standard differences in recovery rates of 2.26, 3.27, and 1.02 mm s^{-1} are measured. Please refer to Supporting Information for more details.

The mold is then cured at 70 °C for 2 h. Upon removal, an outline of the starfish shape is cut from the sheet. The shape outline was chosen to represent a starfish with five legs (Figure 1b). Each leg connects to a circular body of 11 mm in diameter, divided by switching segments of 2 mm width. This diameter was an FDA-approved size for ingestible wireless capsule endoscopes. It is also suitable within a transverse colon, which was

reported to have 50–65 mm diameter. When enclosed in its programmed state, the carrier extends no further than 20 mm in length. The pylorus that connects the stomach to the remainder of the gastrointestinal tract has a diameter of up to 20 mm. Assuming that the carrier is ingested orally, prolonged gastric residence can be avoided by ensuring a smaller diameter during fabrication.

Next, the magnetic composite was made from a mixture of poly-dimethylsiloxane (PDMS) and a ferromagnetic powder with a mean particle size of 5μm (MQFP-16-7-11277, Magnequench GmbH, Germany). The composite mixture was then placed on a similar silicone sheet bracket and heated in an oven at 80 °C for 4 h. The sheet was cut with a laser cutter, placed on top of the SMP layer, and secured with a layer of cyanoacrylate. Furthermore, a Nickel-plated (Ni-Cu-Ni) NdFeB (N50) disc magnet (diameter: 9mm; height: 5 mm) is secured in the center of the SMP body.

Finally, a mixture of gelatin, glycerol, and water was prepared for the biodegradable drug. The ratios for producing this elastomer sample are 1% w/w chemical-grade gelatin and 5% w/w glycerol added to distilled water (6% w/w).[35] Initially, the gelatin was mixed with cold water and allowed to bloom for 30 s. This is followed by mixing the glycerol until the gelatin was thoroughly dispersed. The solution was then heated on a hot plate at 70 °C until the gelatin dissolves fully. Furthermore, a few drops (0.05% w/w) of fluorescein and red acrylic dye are added. The mixture was then heated to 80 °C and mixed until the gelatin was sufficiently dissolved within a transparent solution. Finally, the solution was cooled down to room temperature, and a cube (5 mm^3) is cut from it and placed in the center of the carrier, as shown in **Figure 5**d.

Finite Element Simulation: For the bio-inspired design, the deformation of the structure both in the presence of external magnetic fields and the increasing temperature was simulated using COMSOL Multiphysics (COMSOL Inc., Stockholm, Sweden). The elastic modulus of shape memory material DiAPLEX MP-3510 was set as a function of temperature based on the producer's manual (SMP Technologies Inc., Japan) and previously-reported experimental tests.[54] Two permanent NIB magnets (Supermagnete, Gottmadingen, Germany) were simulated with a remnant flux density of 1.33 T. The larger magnet was 45 mm in diameter and 30mm in height. The simulations were conducted under two conditions: First, moving the magnets' distance d from 20 to 50 mm; and second, increasing the temperature from 20 °C to 50 °C, respectively.

Clinical Application: The carrier was tested for visibility using two imaging modalities. The first was a video gastroscope (i10 Series, Pentax Medical, Dodewaard, the Netherlands) connected to an EPK-100p video processor with a Xenon light source. This gastroscope was the conventional tool for routine lower gastrointestinal tract procedures. Second, the carrier was tested for its compatibility within CT images since the region of the bleeding was sometimes identified through CTA. An Artis Pheno C-beam scanner (Siemens Healthineers, Germany) was used to obtain a 3D volumetric model of the phantom.

Phantom Experimental Setup: A phantom was constructed from PMMA tubes with diameters similar to that of the upper and lower GI tracts. A peristaltic pump was then connected to the tubes and a reservoir of water. The water in placed in a 5 L beaker and heated to a constant temperature of 37 °C using a temperature-controlled laboratory heater. This temperature ensures that the environment within the phantom is consistent with human body temperature. In order to monitor the release rate and size of the drug, an ultraviolet (UV) blacklight projection lamp (Purple Stage Par 65W) is placed below the setup, reflecting the fluorescein ingredient inside the drug.

Before the experiment, the carrier was in its initial (permanent) configuration. Therefore, the carrier shape configuration was first programmed by submerging the carrier in water above T_g (at 50 °C) and subjecting it to mechanical loading on the tip of the legs for 10 s. The carrier was then allowed to cool below T_g, resulting in a programmed, closed state. Next, an operator brings the external magnet close to the insertion orifice and inserted the carrier manually into the tube. The external magnet was used to maneuver the carrier toward a pre-defined target. The permanent shape was then retrieved, followed by shape morphing via magnetic interaction. During this transformation, the simulated drug was monitored until it was completely released. Afterward, the carrier was retrieved by removing it
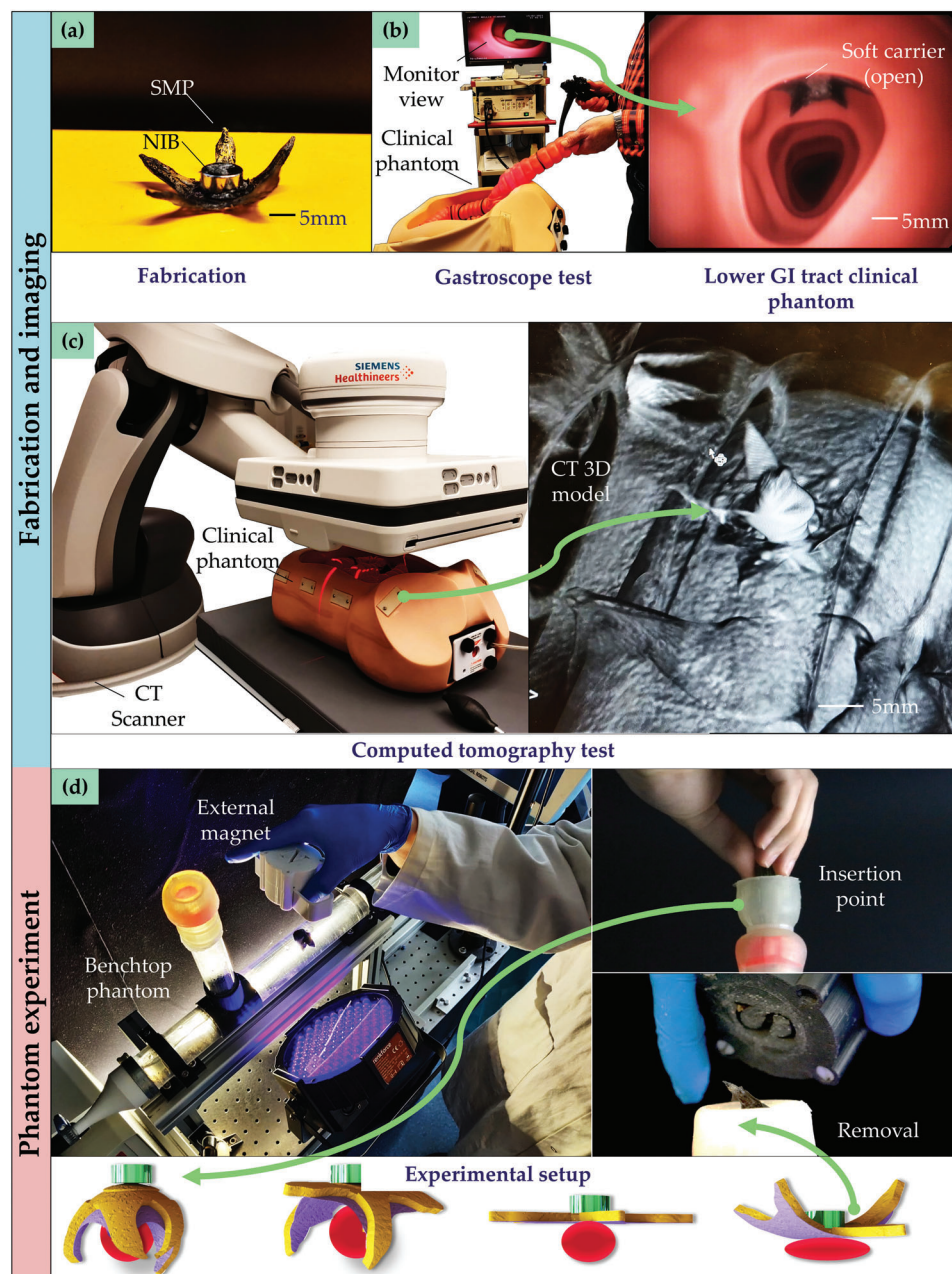
**ADVANCED
SCIENCE NEWS**

www.advancedsciencenews.com

**Macro-
molecular
Bioscience**

www.mbs-journal.de

Figure 5. The experiments for demonstrating the feasibility of the fabricated soft carrier are divided into two phases: Fabrication and imaging—validating its use during interventions that utilize conventional imaging modalities, and Phantom experiment—demonstrating the efficacy of the carrier in a life-size transverse colon phantom. a) The first step is to fabricate the SMP and assemble the multi-layered structure. The soft carrier is then tested within a Hybrid Operating Theatre inside a Computed Tomography (CT) scanner (Artis Pheno, Siemens Healthineers, Erlangen, Germany), with b), a gastroscope, and c) a computed tomography scanner, to ensure it is clinical applicability in terms of its shape, size, and choice of materials. d) A benchtop experiment is set up composed of poly(methyl methacrylate) (PMMA) tubes with diameters similar to those of the upper and lower Gastro-intestinal (GI) tracts of the average human adult. The insertion point represents a natural orifice through which the carrier is inserted manually and also retrieved at the end of the experiment.

from the insertion point using the hand-held magnet (please refer to the accompanying video).

Supporting Information

Supporting Information is available from the Wiley Online Library or from the author.

Acknowledgements

2200559 (8 of 9)

[1] S. Mujtaba, S. Chawla, J. F. Massaad, *J. Clin. Med.* **2020**, *9*, 402.

[2] F. W. Green Jr, M. M. Kaplan, L. E. Curtis, P. H. Levine, *Gastroenterology* **1978**, *74*, 38.

[3] D. Troland, A. Stanley, *Gastrointest. Endosc. Clin.* **2018**, *28*, 277.

[4] D. M. Jensen, S. Eklund, T. Persson, H. Ahlbom, R. Stuart, A. N. Barkun, E. J. Kuipers, J. Mössner, J. Y. Lau, J. J. Sung, J. Kilhamn, T. Lind, *Am. J. Gastroenterol.* **2017**, *112*, 441.

[5] C. Senore, L. Correale, D. Regge, C. Hassan, G. Iussich, M. Silvani, A. Arrigoni, L. Morra, N. Segnan, *Radiology* **2018**, *286*, 873.

[6] K. Jung, W. Moon, *World J. Gastroenterol. Endosc.* **2019**, *11*, 68.

[7] S. I. Rich, R. J. Wood, C. Majidi, *Nat. Electron.* **2018**, *1*, 102.

[8] J. Chan, F. T. Pan, Z. Li, in *13th World Congress on Intelligent Control and Automation (WCICA)*, **2018**, pp. 1366–1369.

[9] S. Filogna, V. Iacovacci, F. Vecchi, L. Musco, A. Menciassi, *Bioinspiration Biomimetics* **2020**, *16*, 026008.

[10] L. Manfredi, E. Capoccia, G. Ciuti, A. Cuschieri, *Sci. Rep.* **2019**, *9*, 1.

[11] V. K. Venkiteswaran, L. F. P. Samaniego, J. Sikorski, S. Misra, *IEEE Robot. Autom. Lett.* **2019**, *4*, 1753.

[12] E. B. Joyee, Y. Pan, *Soft Robot.* **2019**, *6*, 333.

[13] M. Chauhan, J. H. Chandler, A. Jha, V. Subramaniam, K. L. Obstein, P. Valdastri, *Front. Robot. AI* **2021**, *8*, 119.

[14] Q. Ze, S. Wu, J. Nishikawa, J. Dai, Y. Sun, S. Leanza, C. Zemelka, L. S. Novelino, G. H. Paulino, R. R. Zhao, *Sci. Adv.* **2022**, *8*, eabm7834.

[15] L. Ionov, *Adv. Funct. Mater.* **2013**, *23*, 4555.

[16] W. Zhao, L. Liu, F. Zhang, J. Leng, Y. Liu, *Mater. Sci. Eng., C* **2019**, *97*, 864.

[17] B. Q. Y. Chan, Z. W. K. Low, S. J. W. Heng, S. Y. Chan, C. Owh, X. J. Loh, *ACS Appl. Mater. Interfaces* **2016**, *8*, 10070.

[18] Y. Xia, Y. He, F. Zhang, Y. Liu, J. Leng, *Adv. Mater.* **2021**, *33*, 2000713.

[19] M. S. Paolini, O. S. Fenton, C. Bhattacharya, J. L. Andresen, R. Langer, *Biomed. Microdevices* **2019**, *21*, 1.

[20] T. G. Leong, C. L. Randall, B. R. Benson, N. Bassik, G. M. Stern, D. H. Gracias, *Proc. Natl. Acad. Sci.* **2009**, *106*, 703.

[21] W. B. Liechty, D. R. Kryscio, B. V. Slaughter, N. A. Peppas, *Annu. Rev. Chem. Biomol. Eng.* **2010**, *1*, 149.

[22] J. C. Breger, C. Yoon, R. Xiao, H. R. Kwag, M. O. Wang, J. P. Fisher, T. D. Nguyen, D. H. Gracias, *ACS Appl. Mater. Interfaces* **2015**, *7*, 3398.

[23] E. Gultepe, J. S. Randhawa, S. Kadam, S. Yamanaka, F. M. Selaru, E. J. Shin, A. N. Kalloo, D. H. Gracias, *Adv. Mater.* **2013**, *25*, 514.

[24] S. Mishra, *J. Thin Films Coating Sci. Technol. Appl.* **2015**, *2*, 2.

[25] S. Sánchez, W. Xi, A. A. Solovev, L. Soler, V. Magdanz, O. G. Schmidt, in *Small-Scale Robotics. From Nano-to-Millimeter-Sized Robotic Systems and Applications: First International Workshop at ICRA 2013, Karlsruhe, Germany, May 6, 2013, Revised and Extended Papers 1*, Springer, Berlin Heidelberg **2014**, pp. 16–27.

[26] S. Laurent, J.-L. Bridot, L. V. Elst, R. N. Muller, *Future Med. Chem.* **2010**, *2*, 427.

[27] G. Kósa, P. Jakab, G. Székely, N. Hata, *Biomed. Microdevices* **2012**, *14*, 165.

[28] C. Liu, T. Tsao, Y. C. Tai, W. Liu, P. Will, C. M. Ho, in *Proceedings of the Int. Solid-State Sensors Actuators Conf.-TRANSDUCERS'95*, vol. *1*, IEEE, **1995**, pp. 328–331.

[29] J. C. Breger, C. Yoon, R. Xiao, H. R. Kwag, M. O. Wang, J. P. Fisher, T. D. Nguyen, D. H. Gracias, *ACS Appl. Mater. Interfaces* **2015**, *7*, 3398.

[30] S. Miyashita, S. Guitron, M. Ludersdorfer, C. R. Sung, D. Rus, in *2015 IEEE Int. Conf. Robot. Autom. (ICRA)*, IEEE, **2015**, pp. 1490–1496.

[31] A. R. Ahmed, O. C. Gauntlett, G. Camci-Unal, *ACS Omega* **2020**, *6*, 46.

[32] H. Lu, M. Zhang, Y. Yang, Q. Huang, T. Fukuda, Z. Wang, Y. Shen, *Nat. Commun.* **2018**, *9*, 1.

[33] S. Wu, Q. Ze, J. Dai, N. Udipi, G. H. Paulino, R. Zhao, *Proc. Natl. Acad. Sci.* **2021**, *118*, 36.

[34] J. Zhang, Z. Ren, W. Hu, R. H. Soon, I. C. Yasa, Z. Liu, M. Sitti, *Sci. Robot.* **2021**, *6*, eabf0112.

[35] C. Wang, V. R. Puranam, S. Misra, V. K. Venkiteswaran, *IEEE Robot. Autom. Lett.* **2022**, *7*, 5795.

[36] F. Ongaro, S. Scheggi, A. Ghosh, A. Denasi, D. H. Gracias, S. Misra, *PloSone* **2017**, *12*, e0187441.

[37] C. R. Dunn, B. P. Lee, R. M. Rajachar, *Molecules* **2022**, *27*, 5196.

[38] A. Kirillova, L. Ionov, *J. Mater. Chem. B* **2019**, *7*, 1597.

[39] C. M. Heunis, K. J. Behrendt, E. E. Hekman, C. Moers, J.-P. P. de Vries, S. Misra, *IEEE/ASME Trans. Mechatron.* **2021**, *27*, 1761.

[40] M. Runciman, A. Darzi, G. P. Mylonas, *Soft Robot.* **2019**, *6*, 423.

[41] A. Csendes, A. M. Burgos, *Obes. Surg.* **2005**, *15*, 1133.

[42] Q. Zhao, H. J. Qi, T. Xie, *Prog. Polym. Sci.* **2015**, *49*, 79.

[43] Y. Meng, J. Jiang, M. Anthamatten, *J. Polym. Sci., Part B: Polym. Phys.* **2016**, *54*, 1397.

[44] P. Swain, A. Toor, F. Volke, J. Keller, J. Gerber, E. Rabinovitz, R. I. Rothstein, *Gastrointest. Endosc.* **2010**, *71*, 1290.

[45] J. Keller, C. Fibbe, F. Volke, J. Gerber, A. C. Mosse, M. Reimann-Zawadzki, E. Rabinovitz, P. Layer, D. Schmitt, V. Andresen, P. Swain, *Gastrointest. Endosc.* **2011**, *73*, 22.

[46] J.-H. Kim, S.-J. Nam, *Diagnostics* **2021**, *11*, 1792.

[47] O. Erin, M. Boyvat, M. E. Tiryaki, M. Phelan, M. Sitti, *Adv. Intell. Syst.* **2020**, *2*, 1900110.

[48] M. Boyvat, J.-S. Koh, R. J. Wood, *Sci. Robot.* **2017**, *2*, eaan1544.

[49] J. A. Faber, A. F. Arrieta, A. R. Studart, *Science* **2018**, *359*, 1386.

[50] C. O'Shea, Ph.D. Thesis, University College Cork, **2017**.

[51] S. H. Kim, J.-H. Moon, J. H. Kim, S. M. Jeong, S.-H. Lee, *Biomed. Eng. Lett.* **2011**, *1*, 199.

[52] Y. Li, Y.-X. Guo, S. Xiao, *IEEE Trans. Antennas Propag.* **2017**, *65*, 3738.

[53] D. Ling, T. Hyeon, *Small* **2013**, *9*, 1450.

[54] G. Baer, T. Wilson, D. L. Matthews, D. Maitland, *J. Appl. Polym. Sci.* **2007**, *103*, 3882.